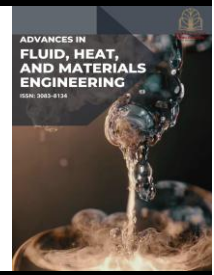




Advances in Fluid, Heat and Materials Engineering

Journal homepage:
<https://karyailham.com.my/index.php/afhme/index>
ISSN: 3083-8134



Analysis of Head Loss in Pipes with Multiple Bends

Muhammad Iqram Hafiz Rusnizam^{1,*}

¹ Department of Mechanical Engineering, Faculty of Mechanical Engineering and Manufacturing, University Tun Hussein Onn Malaysia, 86400 Batu Pahat, Johor, Malaysia

ARTICLE INFO

Article history:

Received 15 October 2025

Received in revised form 12 December 2025

Accepted 15 December 2025

Available online 21 December 2025

Keywords:

Head loss; multiple bend pipe; turbulent flow; computational fluid dynamics (CFD); k- ω SST turbulence model; pressure drops

ABSTRACT

This study investigates the influence of pipe bend spacing on head loss in NPS 2-inch pipes equipped with multiple 90° elbows, a common configuration in compact pipeline systems. Three configurations were examined, where the spacing between consecutive bends was set at 200 mm, 300 mm, and 500 mm, respectively, to assess the impact on flow behaviour and energy losses. Numerical simulations were carried out using ANSYS Fluent, assuming fully turbulent flow with a Reynolds number of approximately 52,000. The k- ω SST turbulence model was applied to capture detailed flow dynamics, including turbulence intensity, pressure distribution, velocity profiles, and energy dissipation mechanisms. A grid independence test was conducted to ensure numerical accuracy, stability, and convergence, validating the chosen mesh size for efficient computational performance. The results revealed that smaller bend spacing significantly increases turbulence kinetic energy (TKE) and pressure losses. Specifically, the 200 mm configuration produced the highest TKE and exhibited an average head loss approximately 18% higher than the 500 mm configuration, with a maximum pressure drop of 312.33 Pa. In contrast, the 500 mm spacing allowed for more uniform flow, reduced turbulence intensity, lower pressure losses, and improved energy efficiency, while the 300 mm configuration showed intermediate behaviour. These outcomes indicate a clear relationship between bend spacing and hydraulic performance, emphasizing that insufficient spacing can lead to higher energy consumption, excessive pressure drops, and reduced pipeline efficiency. The findings provide critical insights for the design and optimization of pipeline systems in industrial applications, particularly where space constraints necessitate multiple bends, guiding engineers to balance compactness with hydraulic performance to achieve efficient, reliable, and cost-effective flow systems.

1. Introduction

This study is about predicting and managing head loss in piping systems, which was a major challenge for engineers, especially in industries that move fluids over long distances or require precise control, such as chemical plants, oil and gas pipelines, and HVAC systems in industrial settings. Head loss is the permanent loss of energy caused by friction, turbulence, secondary flows, and separation within the pipe. When multiple bends are placed close together, these effects become

* Corresponding author.

E-mail address: dd220055@student.uthm.edu.my

<https://doi.org/10.37934/afhme.7.1.112a>

even more complex than a straight pipe system, often resulting in much higher pressure drops and increased energy consumption.

In recent years, advances in computer modelling have allowed researchers to take a fresh look at how fluid behaviour changes as it moves through pipe bends. Studies now emphasize the impact of Dean vortices, which rotate the secondary flows induced by pipe curvature, thereby increasing turbulence and creating uneven velocity profiles inside the bend [1,2]. As fluid moves through a curve at the bends, centrifugal forces push high-momentum fluid toward the outer wall and draw lower-momentum fluid inward, creating pairs of rotating flows in the pipe. These vortex structures stick around downstream of the bend and can interact with other pipe fittings, especially when bends are placed close together.

Past research mostly focuses on single-bend configurations in the pipe. Studies using high-resolution Direct Numerical Simulation (DNS) and Large Eddy Simulation (LES) simulations [3,4] have demonstrated the sensitivity of bend flow to Reynolds number, curvature ratio, and inlet conditions. However, the piping systems with multiple bends, commonly used in industrial installation systems, are not nearly as well-represented in the literature. Existing work shows that turbulence leftover from an upstream bend will influence the flow redevelopment length, wall shear stress, and separation zones in the following bend [5,6]. The interactions can either increase or reduce the flow instabilities, depending on the length between the bends in the pipes.

The increasing use of compact piping arrangements in modern facilities further highlights the need to understand this behaviour. Tight installations in automotive cooling circuits, chemical reactors, and compact heat exchangers often include several of the bends arranged within short distances between bends. Insufficient spacing may lead to turbulence amplification, elevated vibration loads, noise, and increased pumping power demand in the pipe systems. Thus, numerical and experimental investigations of multi-bend systems have become increasingly relevant.

This study builds upon recent developments in turbulence modelling and CFD reliability. The $k-\omega$ SST model has proven accurate for predicting separation and rotation-dominated flows within curved piping systems [7-9]. Combined with mesh refinement strategies and validated hydraulic diameter inputs, it provides a reliable framework for analyzing how the bend pipe spacing affects flow physics. This study evaluates three multi-bend pipe configurations with varying inter-bend lengths at 200 mm, 300mm, and 500 mm to quantify their impact on velocity distribution, pressure fields, and head loss.

2. Methodology

2.1 Geometry Construction

In this study, three-dimensional pipe geometries were developed to analyze the influence of bend spacing on head loss in a multiple-bend piping system. Each configuration consisted of an NPS 2-inch pipe with an internal diameter of 52.48 mm and three consecutive 90-degree bends, all designed with a consistent centerline bend radius of 60.30 mm to ensure uniform curvature effects across all cases. The key difference between the models was the straight-pipe length separating each bend, set to 200 mm, 300 mm, or 500 mm, based on the dimensional data provided in the project specifications. All geometries were constructed with sufficient inlet and outlet extensions to allow the flow to develop before entering the first bend and to stabilize after the final bend, minimizing computational boundary effects. The use of identical pipe diameters and bend radius ensured that differences in hydraulic behaviour could be attributed only to the spacing between bends. This approach allowed a controlled comparison of how geometric layout influences velocity redistribution, turbulence transmission, and overall pressure loss in multiple bend systems, providing a robust foundation for subsequent CFD analysis. Figure 1 displays the geometry of the three multiple

bend pipes, while Figure 2 illustrates the water flow domain, indicating the inlet and outlet boundaries that define the flow direction within the simulation in Ansys, and Table 1 shows the Geometrical properties of multiple bend pipe configurations.

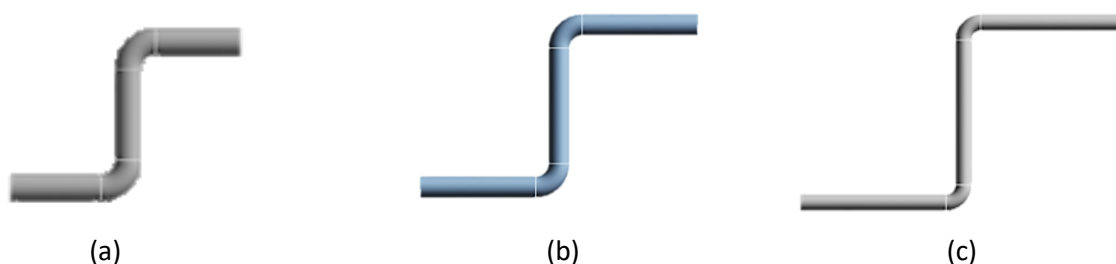


Fig. 1. The geometry of multiple-bending pipe (a) NPS2 200 (b) NPS2 300 (c) NPS2 500

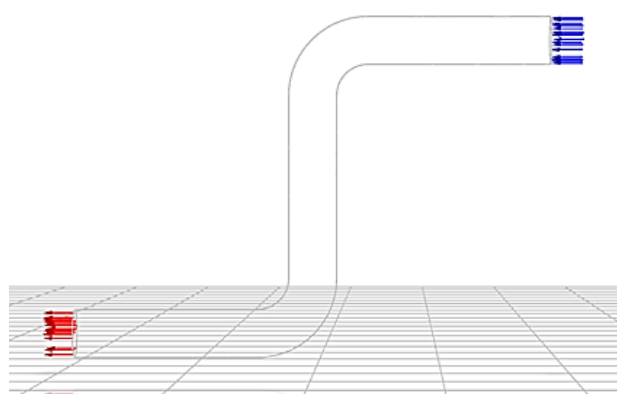


Fig. 2. The geometry of multiple-bending inlet and outlet flow

Table 1

Geometrical properties of multiple bend pipe configurations

Variant	Straight length (mm)	NPS	Internal diameter (mm)	Bend radius (mm)
200 mm	200	2"	52.48	60.30
300 mm	300	2"	52.48	60.30
500 mm	500	2"	52.48	60.30

2.2 Meshing

The meshing process for all three multiple-bend pipe configurations was carried out in ANSYS Meshing using an unstructured tetrahedral mesh, which is commonly used for complex geometries involving curved pipe bends and strong secondary flow structures. A curvature-based Body Sizing control with a curvature normal angle of 10° was applied to ensure that the mesh accurately captured the local geometric variations within each 90-degree elbow. Multiple mesh densities were generated by varying the element size from 2.5 mm to 5 mm, to perform a Grid Independence Test (GIT) and assess the influence of mesh refinement on numerical stability and pressure-drop prediction.

The final selected mesh provided sufficient resolution to capture the development of swirl, flow separation, and secondary vortices commonly observed in curved-pipe turbulence, consistent with recommendations from previous CFD studies on bend-caused flow structures [2-9]. Mesh quality metrics, including skewness and orthogonal quality, were evaluated to ensure fulfillment with ANSYS

Fluent guidelines, and all meshes met the recommended thresholds for accurate pressure-based turbulence modelling.

Figure 3(a) illustrates the tetrahedral mesh distribution across the multiple-bend region, while Figure 3(b) shows a close-up view highlighting element refinement near the curved walls. The chosen mesh successfully balanced computational cost and accuracy, providing reliable flow predictions in agreement with mesh-refinement principles reported in the literature [10].

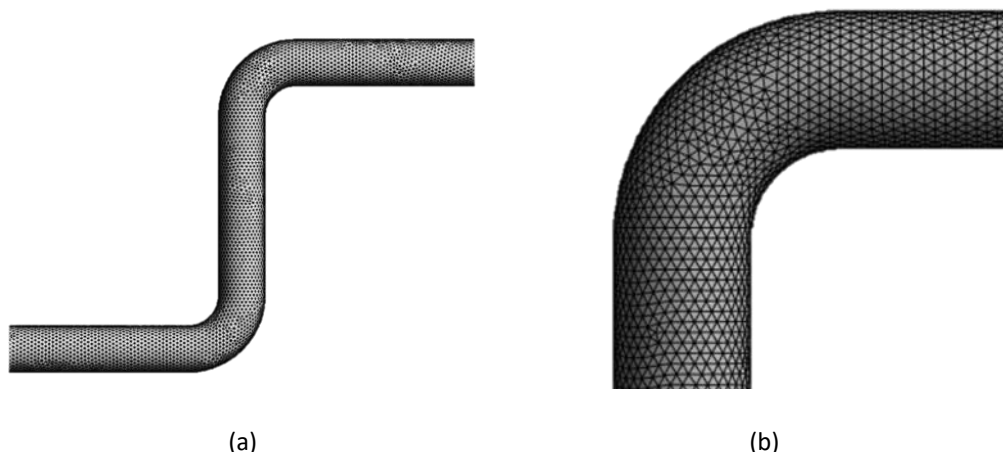


Fig. 3. Meshing for 90-degree bend pipe (a) Meshing at multiple bends (b) Close-up meshing

2.3 Governing Equation

The prediction of head loss in the multiple bend pipe system requires solving the fundamental equations governing incompressible fluid flow. These include the continuity equation, Navier–Stokes momentum equations, and the turbulence transport equations from the $k-\omega$ SST model. Together, these equations allow ANSYS Fluent to simulate pressure, velocity, and turbulence effects within the three-bend pipe configuration [11-15].

2.3.1 Continuity equation (mass conservative)

The continuity equation represents the conservation of mass within a control volume. For incompressible flow, the density remains constant, and the equation simplifies to the requirement that the velocity field must be divergence-free:

$$\nabla \cdot \vec{V} = 0 \quad (1)$$

This condition ensures that the fluid neither accumulates nor loses mass as it passes through each pipe bend. The continuity equation is essential in modelling multi-bend pipes because it preserves a steady volumetric flow rate even when the flow direction changes due to curvature [14-19].

2.3.2 Momentum equation

The momentum equation describes the conservation of linear momentum for a moving fluid. For an incompressible Newtonian fluid, the Navier–Stokes equation is expressed as:

$$\rho(\vec{V} \cdot \nabla)\vec{V} = -\nabla p + \mu \nabla^2 \vec{V} \quad (2)$$

This equation quantifies how pressure forces and viscous effects influence fluid acceleration inside the pipe. In multi-bend systems, the momentum equation is crucial for predicting secondary flows, swirl, and pressure drop caused by curvature, which directly contributes to head loss [9-17-18]

2.3.3 Turbulence transport equation (k - ω SST model)

The k - ω Shear Stress Transport (SST) model provides accurate turbulence prediction for flows involving separation, strong curvature, and adverse pressure gradients, common features in elbow and multi-bend pipes.

2.3.3.1 Turbulence kinetic energy (k) equation

$$\frac{\partial(\rho k)}{\partial t} + \nabla \cdot (\rho k \vec{V}) = P_k - \beta * \rho k \omega + \nabla \cdot [(\mu + \sigma_k \mu_t) \nabla k] \quad (3)$$

This equation models the transport of turbulent kinetic energy within the flow. It is necessary because bend-induced vortices increase turbulence levels, influencing frictional and local losses [3-9].

2.3.3.2 Specific dissipation rate (ω) equation

$$\frac{\partial(\rho \omega)}{\partial t} + \nabla \cdot (\rho \omega \vec{V}) = \alpha \frac{\omega}{k} P_k - \beta \rho \omega^2 + \nabla \cdot [(\mu + \sigma_\omega \mu_t) \nabla \omega] \quad (4)$$

This equation determines the rate at which turbulence dissipates. It is important because flow separation at the bends significantly increases turbulence generation, affecting the predicted pressure losses [3-9].

2.3.4 Head loss equation

The head loss represents the energy loss due to friction and turbulence caused by pipe bends. The pressure drop obtained from CFD is converted into hydraulic head loss using:

$$h_L = \frac{\Delta P}{\rho g} \quad (5)$$

This equation allows comparison of energy losses between the three geometric variants NPS2–200 mm, NPS2–300 mm, and NPS2–500 mm, and is standard in engineering pipe-flow analysis [3-9].

2.3.5 Loss coefficient (minor loss) equation

The loss coefficient (K) quantifies the bend-induced energy loss independent of pipe size. This is required because head loss alone cannot compare losses between geometries. K validates the pressure drop using dynamic pressure, making results comparable across all pipe bend configurations [20-22].

$$K = \frac{\Delta P}{\frac{1}{2}\rho V^2} \quad (6)$$

2.4 Boundary Condition & Parameter Assumption

The CFD simulations in this study were performed using water at room temperature under steady-state and incompressible flow conditions. These assumptions are commonly used in internal pipe-flow simulations, especially for analysing flow behaviour in bends and elbows pipe systems [11-23]. The main boundary conditions applied in this work are velocity inlet, pressure outlet, and no-slip walls are summarised clearly in Table 2, which provides an overview of all parameters used in the setup in Ansys Fluent. A no-slip condition is applied on all pipe walls, meaning that the fluid velocity is zero at the surface. This boundary condition is essential for predicting frictional losses and wall shear stress accurately. The past studies show that the no-slip assumption is crucial when calculating head loss in bends and curved pipes [24,25].

At the inlet, a uniform velocity of 1.0 m/s is standard for all three configurations. Using the same inlet velocity helps to ensure a consistent Reynolds number and allows a fair comparison regarding how bend length affects pressure loss in this case study. This approach follows recommendations from previous CFD studies evaluating geometric influence on minor losses [26]. For turbulence modelling, the SST k- ω model is used because it performs well in flows with curvature, separation, and secondary vortices phenomena that strongly influence energy losses in 90° bends [19-27]. This model has been widely validated for multiple bend internal flow analysis.

At the outlet, a 0 Pa gauge pressure boundary condition is assigned. This serves as a reference plane for static pressure measurement, and it is a standard setup in many CFD studies that investigate head loss in pipelines with sudden or progressive geometric changes [28,29].

Table 2

Boundary conditions for CFD simulation

Boundary	Type	Specification	Value
Inlet	Velocity inlet	Velocity	10 m/s
		Turbulence intensity	5%
		Hydraulic diameter	0.05248 m
Outlet	Pressure outlet	Gauge pressure	0 Pa
Wall	No-slip	Smooth	Stationary

3. Results

3.1 Grid Independence Test (GIT)

The Grid Independence Test (GIT) was conducted to determine the mesh truncation error that yields accurate, stable numerical results at a reasonable computational cost. In CFD simulations involving pipe bends, mesh refinement is significant because the curved geometry produces secondary flows, velocity skewing, and pressure gradients that must be properly captured by the sampled domain [5]. For this study, Body Sizing values ranging from 2.5 to 5.0 were tested, corresponding to element counts between 938,746 and 126,604. The objective of the GIT is to ensure that variations in mesh sizing method do not significantly influence key output parameters, especially the pressure difference (ΔP), which is essential for calculating head loss in multiple bend pipes.

Table 3 presents the complete GIT dataset, including static pressure, total pressure, velocity magnitude at major flow locations (inlet, outlet, and wall), and truncation error. As shown in Table 3, coarse meshes that contain body sizes 2.5-3.5 produced noticeably higher-pressure differences, with

the difference pressure ΔP reducing from 312.33 Pa for body sizing 2.5 mm to 291.84 Pa for body sizing 3.5 mm. As the mesh was refined further, the pressure difference approached a converged value. For body sizing 4.75 mm, the pressure difference ΔP was 284.52 Pa, with a low truncation error of 0.3648%, indicating grid-independent behaviour. The refinement trend follows common CFD observations, where the solution stabilises once near-wall gradients and curvature-induced flow separations are sufficiently resolved [30,31].

Figure 2 shows the mesh distribution for the multiple-bend pipe. The curvature-normal angle of 10° generates finer elements along the bend, improving the resolution of the centrifugal flow effects. This treatment is consistent with best practices for meshing curved pipe geometries, where smooth transitions and local refinement are required to capture Dean vortices and wall shear distribution [19]. The velocity magnitude values across different meshes also show tight convergence, indicating a stable representation of the flow field. For example, all meshes predict an inlet velocity magnitude of approximately 1 m/s, with outlet velocities varying only in the 1.003-1.005 m/s range, showing minimal sensitivity to mesh refinement.

Based on the results, body sizing 4.75 mm is selected as the optimal mesh for this study. Although the body sizing 4.5 mm mesh also performed well, the body sizing 4.75 mm mesh produced the lowest truncation error and a pressure difference ΔP value that remained consistent with finer meshes, while requiring fewer elements and computational resources. According to modern CFD grid-selection guidelines, the ideal mesh is one in which further refinement yields decreasing improvements and stable output behaviour [19]. Therefore, the body sizing 4.75 mm configuration provides the best balance between accuracy and efficiency for head-loss simulation in multiple bend pipes.

Table 3

Grid independence test (GIT) variable for mesh statistics and pressure-based truncation error

Body sizing	Element	Node	Inlet	Outlet	ΔP	Truncation error
2.5	938,746	169,837	312.33278	0	312.33278	
3	545,605	100,274	300.76946	0	300.76946	3.702243485
3.5	345,758	64,568	291.84142	0	291.84142	2.968399784
4	232,581	44,136	286.84547	0	286.84547	1.711871468
4.5	162,027	31,077	285.56445	0	285.56445	0.44658889
4.75	140,369	27,325	284.52268	0	284.52268	0.364810816
5	126,604	24,999	286.19395	0	286.19395	0.587394298

3.2 Solver Setting

The simulations were run using a pressure-based steady solver. The $k-\omega$ SST turbulence model was used to capture flow separation and swirl. SIMPLE was used for pressure-velocity coupling, and second-order upwind schemes were applied for momentum and turbulence equations. Hybrid initialization was used, and convergence criteria were set as 1×10^{-4} for continuity and momentum, and 1×10^{-5} for turbulence variables. Monitors were created to track pressure difference, mass flow, and velocity along the pipe centerline. The detailed solver settings used in the simulations are summarized in Table 4.

Table 4

Fluent setup for solver settings

Setting	Setup
General	Pressure-based Steady Absolute
Method	SIMPLE Least squares cell-based Second-order discretization for all variables
Initialize	Hybrid initialization
Run calculation	Check case Iteration 2000

3.1 Pressure

Pressure distribution is the primary parameter used to evaluate energy loss and flow resistance in internal pipe flows. In this study, pressure contours are analysed for three different pipe centerline spacing configurations for straight pipe before bending, 200 mm, 300 mm, and 500 mm, under turbulent conditions with a fixed pressure outlet. The pressure contours show a clear drop after every bend, with the largest pressure losses occurring in the 200 mm system. The shorter spacing between bends limits the recovery of the flow, causing higher resistance and a greater overall pressure drop. The 300 mm system exhibits a moderate pressure decrease, while the 500 mm system has the lowest pressure loss due to smoother flow redevelopment. Pressure dropped sharply after each bend, and the shortest-spacing model, NPS2-200 mm, recorded the highest-pressure difference ΔP . Consequently, the calculated head loss trend was $h_{L,200} > h_{L,300} > h_{L,500}$.

Figure 4 illustrates the pressure contours for the three configurations using a global pressure range between minimum: -760.996 Pa, maximum: 488.252 Pa, while Figure 5 presents a zoomed-in view using a user-specific pressure range that has a minimum: -3 Pa, and maximum: 3 Pa. Lastly, the detailed solver settings used for the simulations are summarized in Table 4.

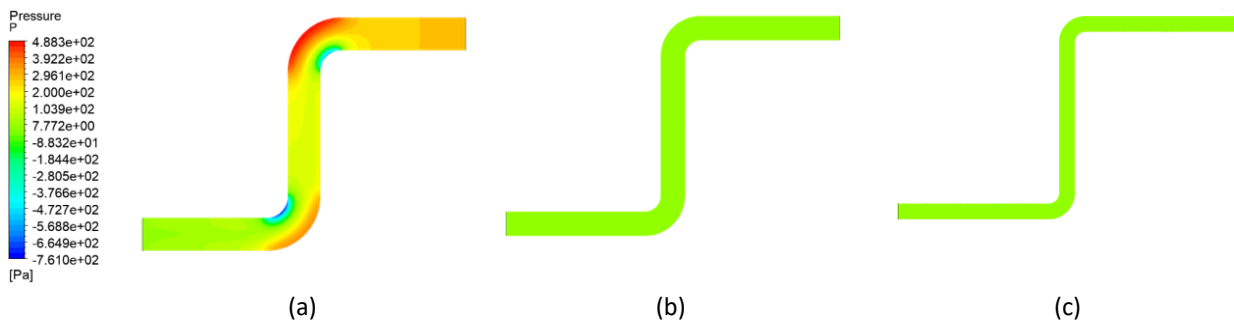


Fig. 4. Using a pressure range Global min: -760.996 Pa, max: 488.252 Pa for (a) NPS2 200 (b) NPS2 300 (c) NPS2 500

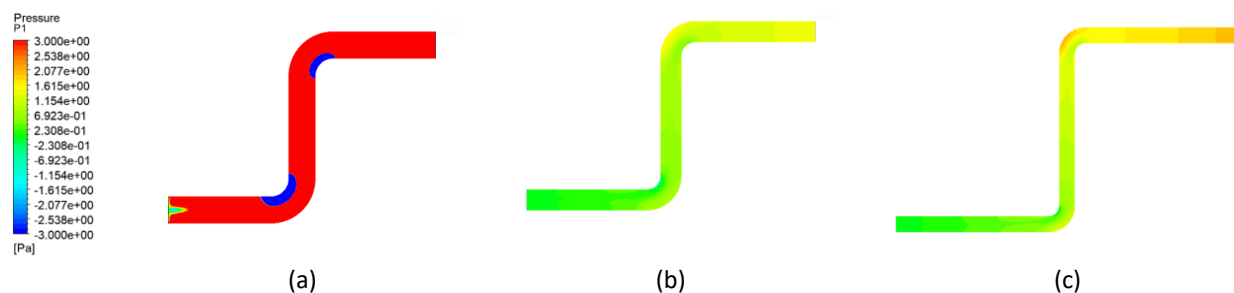


Fig. 5. Using a pressure range user-specific min: -3 Pa, max: 3 Pa for (a) NPS2 200 (b) NPS2 300 (c) NPS2 500

The observed tendency of a smaller effective diameter or more abrupt geometrical changes causing larger pressure loss is consistent with recent CFD studies. For instance, a study on turbulent flow in pipe bends using CFD found that flow curvature and bend geometry substantially influence static pressure distribution and energy losses [11].

3.2 Velocity

Velocity distribution is an important parameter to understand the flow behaviour inside the pipe systems. It shows how fluid moves through bends and straight sections, including areas of swirl and recirculation. In this study, velocity contours were analysed for three pipe centerline spacing configurations at 200 mm, 300 mm, and 500 mm under turbulent flow conditions. In the 200 mm configuration, the flow entering each bend is still affected by the swirl from the previous bend. This creates asymmetrical velocity profiles, higher peak velocities along the inner bend wall, and larger recirculation zones. The 300 mm configuration shows moderate redevelopment of the flow between bends. The 500 mm configuration has the most stable velocity profile before entering the next bend. The flow has more time to redevelop along the longer straight sections. This reduces swirl interactions and results in a more uniform velocity distribution. The main observations are asymmetrical velocity profiles, high peak velocities near the inner wall, and extended recirculation zones. The velocity contours for all three configurations are shown in Figure 6. The results agree with previous CFD studies, which show that pipe curvature and short straight sections increase velocity distortion and recirculation in bends [11].

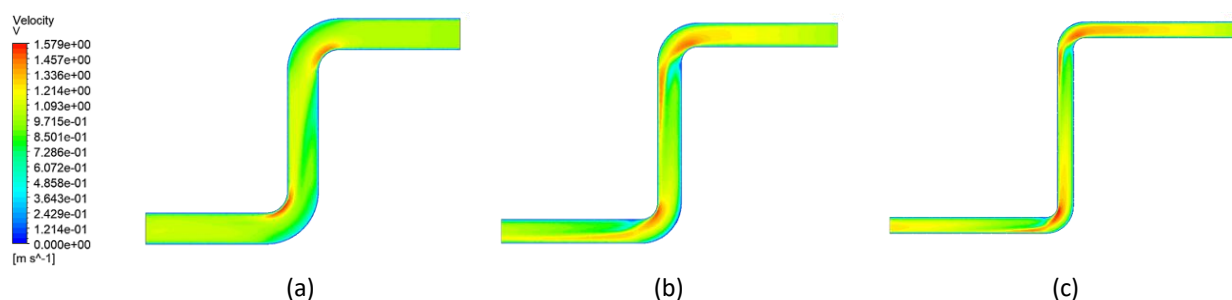


Fig. 6. Using a velocity range global min: 0 ms⁻¹, max: 1.57869 ms⁻¹ for (a) NPS2 200 (b) NPS2 300 (c) NPS2 500

3.2 Turbulent Kinetic Energy

Turbulent kinetic energy (TKE) represents the intensity of velocity changes in a turbulent flow and is directly linked to turbulence production and energy dissipation. In this study, TKE contours were analysed for the three pipe-centreline spacing configurations are 200 mm, 300 mm, and 500 mm. The Turbulent Kinetic Energy TKE distribution provides insight into how bend spacing affects turbulence generation in bent pipes.

Figure 7 shows the Turbulence Kinetic Energy TKE contours for all three configurations, with a minimum value of 3.1×10^{-4} and a maximum value of $4.487 \times 10^{-2} \text{ m}^2/\text{s}^2$. In the 200 mm configuration, Turbulence Kinetic Energy TKE is concentrated near the inner bend wall and within the recirculation zones, indicating strong turbulence production due to high velocity gradients and swirl interactions from successive bends [11].

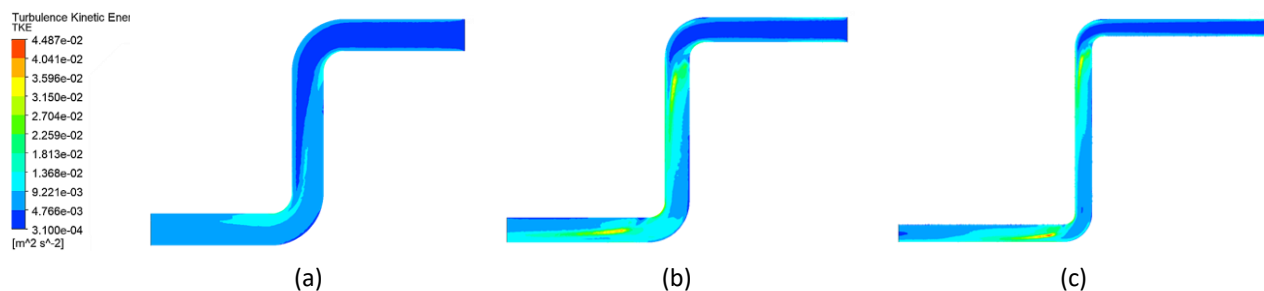


Fig. 7. Using a turbulent kinetic energy range global min: $3.1 \times 10^{-4} \text{ m}^2/\text{s}^2$, max: $4.487 \times 10^{-2} \text{ m}^2/\text{s}^2$ for (a) NPS2 200 (b) NPS2 300 (c) NPS2 500

In the 300 mm configuration, Turbulence Kinetic Energy TKE is lower compared to the 200 mm case, as the flow has more distance to re-develop between bends. This reduces swirl intensity and turbulence production. The 500 mm configuration shows the lowest Turbulence Kinetic Energy TKE among all cases, with a more uniform distribution along the pipe. The longer straight length allows the flow to stabilise and dissipate turbulent fluctuations, resulting in weaker energy dissipation. These observations are consistent with previous CFD studies of turbulent flow in pipe bends, which reported that tighter curvature or shorter spacing between bends increases TKE near the wall and in recirculation zones, whereas longer straight sections reduce turbulence intensity [11-13]. The detailed Turbulence Kinetic Energy TKE contours are presented in Figure 7.

4. Conclusions

The results of this study clearly demonstrate that the spacing between multiple bends in a piping system has a significant impact on head loss, turbulence characteristics, and overall flow efficiency. The 200 mm spacing configuration generated the highest turbulence and pressure drop, with a recorded pressure difference (ΔP) of 312.33 Pa, which is approximately 9.6% higher than the 500 mm configuration $\Delta P = 284.52 \text{ Pa}$, making it the least energy-efficient design. This increase was mainly caused by the amplification of turbulence and swirl effects, leading to significant flow separation and higher energy dissipation. The 300 mm configuration exhibited intermediate behaviour, with a pressure difference ΔP of 291.84 Pa, representing a 2.5% decrease from the 200 mm case but still higher than the 500 mm configuration. Regarding velocity, the 200 mm configuration showed slightly higher peak velocity magnitude at the bends, about 1.4% higher than the 500 mm configuration, due to accelerated flow in regions of strong curvature. Similarly, turbulence kinetic energy (TKE) was highest in the 200 mm spacing, reaching a maximum of 4.487×10^{-2} , which is approximately 18% higher than the 500 mm configuration, indicating more intense turbulence and energy dissipation.

In contrast, the 500 mm configuration exhibited more stable flow with reduced turbulence than other bends, lower turbulence kinetic energy TKE, and a more uniform velocity profile, which contributed to minimized pressure losses and improved energy efficiency. These findings highlight the critical importance of considering bend spacing in the design of piping systems, particularly for industrial applications where minimizing energy consumption, reducing pumping power, and enhancing flow stability are crucial. For systems requiring multiple directional changes, longer straight sections between bends are recommended to optimize hydraulic performance, reduce turbulence-induced losses, and improve overall operational efficiency.

References

- [1] Kalpakli Vester, Athanasia, Ramis Örlü, and P. Henrik Alfredsson. "Turbulent flows in curved pipes: Recent advances in experiments and simulations." *Applied Mechanics Reviews* 68, no. 5 (2016): 050802. <https://doi.org/10.1115/1.4034135>

- [2] Dutta, Prasun, Naveen Kumar Rajendran, Robert Cep, Rakesh Kumar, Himanshu Kumar, and Yadaiah Nirsanametla. "Numerical investigation of Dean vortex evolution in turbulent flow through 90° pipe bends." *Frontiers in Mechanical Engineering* 11 (2025): 1405148. <https://doi.org/10.3389/fmech.2025.1405148>
- [3] Dutta, Prasun, Himadri Chattopadhyay, and Nityananda Nandi. "Numerical studies on turbulent flow field in a 90 deg pipe bend." *Journal of Fluids Engineering* 144, no. 6 (2022): 061104. <https://doi.org/10.1115/1.4053547>
- [4] Ayala, O., G. Rivera-Hernández, and C. Knight. "Computational fluid dynamics study of the effects of secondary flows in 90-degree pipe elbow erosion." In *Comsol Conference* (2020): 2-4.
- [5] Yang, Qi, Jie Dong, Tongju Xing, Yi Zhang, Yong Guan, Xiaoli Liu, Ye Tian, and Peng Yu. "RANS-based modelling of turbulent flow in submarine pipe bends: Effect of computational mesh and turbulence modelling." *Journal of Marine Science and Engineering* 11, no. 2 (2023): 336. <https://doi.org/10.3390/jmse11020336>
- [6] Zardin, Barbara, Giovanni Cillo, Carlo Alberto Rinaldini, Enrico Mattarelli, and Massimo Borghi. "Pressure losses in hydraulic manifolds." *Energies* 10, no. 3 (2017): 310. <https://doi.org/10.3390/en10030310>
- [7] Toumey, Julian, Peiyu Zhang, Redjem Hadeff, and Xinyu Zhao. "Assessment of turbulence models for simulating confined swirling flows." In *Spring Technical Meeting Eastern States Section of the Combustion Institute, Columbia, South Carolina*. 2020.
- [9] Apalowo, Rilwan. "Numerical study of different models for turbulent flow in a 90° pipe bend." *U. Porto Journal of Engineering*, 2022. https://doi.org/10.24840/2183-6493_008.002_0010
- [10] Zulkifli, Zulaika, NH Abdul Halim, Z. H. Solihin, J. Saedon, A. A. Ahmad, A. H. Abdullah, N. Abdul Raof, and M. Abdul Hadi. "The analysis of grid independence study in continuous disperse of MQL delivery system." *Journal of Mechanical Engineering and Sciences* (2023): 9586-9596. <https://doi.org/10.15282/jmes.17.3.2023.5.0759>
- [11] Apalowo, Rilwan Kayode, and Cletus John Akisin. "CFD-based investigation of turbulent flow behavior in 90-deg pipe bends." *Journal of Applied Research in Technology & Engineering* 5, no. 2 (2024): 53-62. <https://doi.org/10.4995/jarte.2024.20665>
- [12] Wang, Liwei, Dianrong Gao, and Yigong Zhang. "Numerical simulation of turbulent flow of hydraulic oil through 90° circular-sectional bend." *Chinese Journal of Mechanical Engineering* 25, no. 5 (2012): 905-910. <https://doi.org/10.3901/CJME.2012.05.905>
- [13] Jain, Paras, Amitava Choudhury, Prasun Dutta, Kanak Kalita, and Paolo Barsocchi. "Random forest regression-based machine learning model for accurate estimation of fluid flow in curved pipes." *Processes* 9, no. 11 (2021): 2095. <https://doi.org/10.3390/pr9112095>
- [14] Cengel, Yunus, and John Cimbala. *Ebook: Fluid mechanics fundamentals and applications (si units)*. McGraw Hill, 2013.
- [15] Anderson, John David, Gérard Degrez, Erik Dick, and Roger Grundmann. *Computational fluid dynamics: an introduction*. Springer Science & Business Media, 2013.
- [16] Kundu, Pijush K., Ira M. Cohen, David R. Dowling, and Jesse Capecelatro. *Fluid mechanics*. Elsevier, 2024.
- [17] Gajbhiye, Bhavesh D., Harshawardhan A. Kulkarni, Shashank S. Tiwari, and Channamallikarjun S. Mathpati. "Teaching turbulent flow through pipe fittings using computational fluid dynamics approach." *Engineering Reports* 2, no. 1 (2020): e12093. <https://doi.org/10.1002/eng2.12093>
- [18] You, Rui, and Nathan H. Kennedy. "A combined CFD, theoretical, and experimental approach for improved hydrodynamic performance of a clam dredge system." *Journal of Marine Science and Engineering* 13, no. 7 (2025): 1305. <https://doi.org/10.3390/jmse13071305>
- [19] Widiawaty, C. D., A. I. Siswantara, G. G. R. Gunadi, H. Pujowidodo, and M. H. G. Syafei. "A CFD simulation and experimental study: predicting heat transfer performance using SST k- ω turbulence model." In *IOP Conference Series: Materials Science and Engineering*, 909, no. 1, p. 012004. IOP Publishing, 2020. <https://doi.org/10.1088/1757-899X/909/1/012004>
- [20] Bibok, Máté, Péter Cszmadia, and Sára Till. "Experimental and numerical investigation of the loss coefficient of a 90 pipe bend for power-law fluid." *Periodica Polytechnica Chemical Engineering* 64, no. 4 (2020): 469-478. <https://doi.org/10.3311/PPCh.14346>
- [22] Kudela, Henryk. "Hydraulic losses in pipes." *Wroclaw University of Science and* (2012): 39.
- [23] Abuhatira, A., S. M. Salim, and J. B. Vorstius. "Numerical simulation of turbulent pipe flow with elbow bend: comparison between RANS and LES." In *32nd Scottish Fluid Mechanics Meeting*, pp. 25-25. University of Dundee, 2019.
- [24] Majdalani, Joseph. "In Memoriam: Frank M. White (1933–2022)." *Journal of Fluids Engineering* 144, no. 11 (2022): 110101. <https://doi.org/10.1115/1.4055275>
- [25] Prabhakara, Sandeep, and M. D. Deshpande. "The no-slip boundary condition in fluid mechanics: 1. The riddle of fluid sticking to the wall in flow." *Resonance* 9, no. 4 (2004): 50-60. <https://doi.org/10.1007/BF02834856>

- [26] Rao, B. Joga, Nakkina VVS Sekhar, Bommina Kumara Swamy, Madam Sai Sandeep, and Kona Hari Babu. "Fabrication, design and analysis of minor losses in pipe." *International Journal for Modern Trends in Science and Technology* 8, no. S06 (2022): 152-157.
- [27] Menter, Florian R. "Two-equation eddy-viscosity turbulence models for engineering applications." *AIAA journal* 32, no. 8 (1994): 1598-1605. <https://doi.org/10.2514/3.12149>
- [28] Fan, Qinyin. *CFD simulation of pressure drop in line pipe*. No. 2006-01-1443. SAE Technical Paper, 2006. <https://doi.org/10.4271/2006-01-1443>
- [29] Madhavan, Sudharsan, and Erica M. Cherry Kemmerling. "The effect of inlet and outlet boundary conditions in image-based CFD modeling of aortic flow." *Biomedical Engineering Online* 17, no. 1 (2018): 66. <https://doi.org/10.1186/s12938-018-0497-1>
- [30] Martins, Nuno MC, Nelson JG Carrico, Helena M. Ramos, and Didia IC Covas. "Velocity-distribution in pressurized pipe flow using CFD: Accuracy and mesh analysis." *Computers & Fluids* 105 (2014): 218-230. <https://doi.org/10.1016/j.compfluid.2014.09.031>
- [31] Chawner, John R., John Dannenhoffer, and Nigel J. Taylor. "Geometry, mesh generation, and the CFD 2030 vision." In *46th AIAA Fluid Dynamics Conference*, p. 3485. 2016. <https://doi.org/10.2514/6.2016-3485>